

Abundant intrinsic heavy sea quarks in the proton and their phenomenological implication

Susumu Koretune

Department of Physics, Fukui Medical School, Matsuoka, Fukui, 910-11, Japan

(Received 10 August 1994)

It is shown that heavy sea quarks such as the charm, bottom, and top quarks intrinsic to the proton exist abundantly in the small x region. The sum rule to test this phenomenon directly is proposed. Then by taking the total cross-section rise in the hadron reactions into account with the use of the soft Pomeron by Donnachie and Landshoff, we show that the rapid rise observed at DESY HERA below $x=0.01$ may be related to this abundance. Further, the constraints at low x which lead to this are matched to the perturbative leading twist behavior and the qualitative behavior of the structure function at low x is studied.

PACS number(s): 13.60.Hb, 11.55.Hx, 12.38.Lg

I. INTRODUCTION

Recently the data of the proton structure function F_2 in the small x region at the DESY ep collider HERA has been reported [1]. Though there still exist large errors, a rapid rise of it with decreasing x and the large rapidity gap events which suggest the existence of the Pomeron component are very interesting. Concerning the rapid rise, we cannot know whether or not this rise continues into the smaller x region, but the behavior near the region $x = 10^{-3}$ – 10^{-2} reminds us of the hard Pomeron [Balitsky-Fadin-Kuraev-Lipatov (BFKL) Pomeron] [2], i.e., $F_2 \sim x^{-\lambda}$ with a relatively large λ . Then phenomenological analyses based on the BFKL equation [3] or Altarelli-Parisi Q^2 evolution with a BFKL-motivated input distribution [4] have been given. Since both the statistical and the systematical errors are large, the distinction between these approaches are difficult [5]. On the other hand, the BFKL approach has serious ambiguities as to the treatment of the nonperturbative region [3]. In view of these situations, it is important to investigate whether or not there exist nonperturbative physical reasons to give such BFKL-like steep behavior. The purpose of this paper is to give such an example.

Our approach is based on the soft Pomeron proposed by Donnachie and Landshoff [6] combined with the sum rules based on the current anticommutation relations on the null plane [7,8]. The modified Gottfried sum rule [9] which explains the experimental value of the New Muon Collaboration (NMC) is one example of these sum rules; hence, this method stands on the same theoretical footing as this sum rule. Let us explain the facts. In the course of the derivation of the modified Gottfried sum rule, we obtained the constraint that the residue of the Pomeron in the πN total cross section is related to the small x limit of the structure function F_2 . The assumption to reach this result was that the trajectory of the Pomeron $\alpha_P(t)$ satisfies $\alpha_P(t) < 1$ at some small t [8]. A simple moving pole in [6] satisfies this criterion. Even when both the hard and the soft Pomeron exist, the heterotic Pomeron may become a simple moving pole [10].

In such a case this criterion may also be satisfied. In this sense this method does not necessarily contradict with BFKL method. Now by this constraint we obtain the theorem that no Q^2 scale exists where we can neglect the sea quark as long as it has a soft Pomeron piece. This theorem may be discarded effectively if the soft Pomeron component is restricted only in the very small x region where experiments cannot reach. However for the light sea quarks we already know that we cannot discard it. This was the very reason why the Gottfried sum rule was badly broken and should be modified as in [9]. Now since the soft Pomeron piece enters every sea quark uniformly, for heavy sea quarks we expect that this theorem also cannot be discarded. Then we transform the sum rules into the ones for the sea quarks and show that the heavy sea quarks intrinsic to the proton are abundant in the small x region. We explain these things in Sec. II. In Sec. III, we study how the nonperturbative constraints match the perturbative Q^2 dependence by a simple toy model. In so doing we explain another origin of the Q^2 dependence. This comes from the structure of the Pomeron and in the present stage of the theory this is completely unknown. Then we show that the abundance of the heavy sea quarks effectively produces the behavior $F_2 \sim x^{-\lambda}$ as in the hard Pomeron and that it may be related to the rapid rise observed at HERA. The discussions are given in Sec. IV. A review of the derivation of the current anticommutator on the null plane is given in Appendix A. Sum rules for SU(5) and SU(6) are explicitly given in Appendix B, and some discussion which suggests the intimate relation between low and high energies is given in Appendix C.

II. THE DERIVATION OF THE NONPERTURBATIVE CONSTRAINTS ON THE SEA QUARKS AND THE SUM RULES FOR THEM

Many years ago the hadronic matrix element of the current anticommutation relations on the null plane were proposed as [7]

$$\begin{aligned} \langle p | \{ J_a^+(x), J_b^+(0) \} | p \rangle_c \delta(x^+) &= \langle p | \{ J_a^{5+}(x), J_b^{5+}(0) \} | p \rangle_c \delta(x^+) \\ &= \frac{1}{\pi} P \left(\frac{1}{x^-} \right) \delta^2(\vec{x}^\perp) \delta(x^+) [d_{abc} A_c(p \cdot x, x^2 = 0) + f_{abc} S_c(p \cdot x, x^2 = 0)] p^+, \end{aligned} \quad (1)$$

where c means to take the connected matrix element and the state $|p\rangle$ is the stable one-particle state. This relation was derived by using the Deser-Gilbert-Sudarshan representation [11], the spectral condition of the hadrons, and the current commutation relations on the null plane. Using a standard method to get the fixed-mass sum rule on the null plane [12], we can get many sum rules from relation (1). All these sum rules come from the d_{abc} term in it (for a review of the derivation of the relation (1) see Appendix A). Setting aside the question of convergence, they are given simply as

$$g_A^2(0) + \frac{2f_\pi^2}{\pi} \int_{\nu_0^p}^{\infty} \frac{d\nu}{\nu} \{ \sigma^{\pi^+ p}(\nu) + \sigma^{\pi^- p}(\nu) \} = \frac{1}{2\pi} P \int_{-\infty}^{\infty} \frac{d\alpha}{\alpha} \sum_i a_i A_i(\alpha, 0), \quad (2)$$

$$\int_0^1 \frac{dx}{2x} \{ F_2^{\nu p}(x, Q^2) + F_2^{\nu \bar{p}}(x, Q^2) \} = \frac{1}{2\pi} P \int_{-\infty}^{\infty} \frac{d\alpha}{\alpha} \sum_i b_i A_i(\alpha, 0), \quad (3)$$

$$\int_0^1 \frac{dx}{x} F_2^{ep}(x, Q^2) = \frac{1}{18\pi} P \int_{-\infty}^{\infty} \frac{d\alpha}{\alpha} \sum_i c_i A_i(\alpha, 0), \quad (4)$$

$$\int_0^1 \frac{dx}{x} F_2^{en}(x, Q^2) = \frac{1}{18\pi} P \int_{-\infty}^{\infty} \frac{d\alpha}{\alpha} \sum_i d_i A_i(\alpha, 0), \quad (5)$$

$$[g_A^{p\Sigma^0}(0)]^2 + [g_A^{p\Lambda}(0)]^2 + U_p + \frac{2f_K^2}{\pi} \int_{\nu_0^K}^{\infty} \frac{d\nu}{\nu} [\sigma^{K^+ p}(\nu) + \sigma^{K^- p}(\nu)] = \frac{1}{2\pi} P \int_{-\infty}^{\infty} \frac{d\alpha}{\alpha} \sum_i e_i A_i(\alpha, 0), \quad (6)$$

$$[g_A^{n\Sigma^-}(0)]^2 + U_n + \frac{2f_K^2}{\pi} \int_{\nu_0^K}^{\infty} \frac{d\nu}{\nu} [\sigma^{K^+ n}(\nu) + \sigma^{K^- n}(\nu)] = \frac{1}{2\pi} P \int_{-\infty}^{\infty} \frac{d\alpha}{\alpha} \sum_i f_i A_i(\alpha, 0), \quad (7)$$

where σ^{ab} means the total cross section of the ab scattering at $q^2 = 0$, ν_0 means the threshold in each reaction, U_p and U_n are the contributions below the threshold, and $\nu = p \cdot q$. Only the coefficients of the diagonal matrix elements are not zero. Table I summarizes these coefficients.

Table I should be read as follows. For SU(3) the suffix i stops at 8 and the zeroth component is given by the one at the column 0 (3). The cases of 4,5,6 flavors are read similarly. Except for the zeroth component, each coefficient is unchanged when the flavor symmetry group is enlarged. This simple rule has a clear physical meaning in the parton language. For example, in the case SU(3) \rightarrow SU(4), the distribution of the charm sea quark is added to the ones of up, down, and strange sea quarks without

changing anything of them. We will come back to this fact later in this section. Now the coefficient b_i is given as follows. For SU(3), we obtain $b_0 = 2\sqrt{6}/3$, $b_3 = 0$, $b_8 = 2\sqrt{3}/3$. For SU(4), $b_0 = 2\sqrt{2}$, $b_3 = b_8 = b_{15} = 0$. For SU(5), $b_0 = 4\sqrt{10}/5$, $b_3 = b_8 = 0$, $b_{24} = 2\sqrt{10}/5$. For SU(6), $b_0 = 2\sqrt{3}$, $b_3 = b_8 = b_{15} = b_{35} = 0$. This complexity arises from an asymmetrical treatment of the charged weak currents in the cases SU(3) and SU(5). In spite of this, if we look into the sum rules we will find that the change of b_i is made such that the interpretation by the parton language as mentioned above is maintained.

Now before going into the details we first explain a flavor symmetry group such as SU(4), SU(5), and SU(6).

TABLE I. Coefficients a_i, c_i, d_i, e_i, f_i , where $0(N)$ means the zeroth component for SU(N).

| i | 0(3) | 0(4) | 0(5) | 0(6) | 3 | 8 | 15 | 24 | 35 |
|-------|---------------|-------------|-----------------|---------------|----|---------------|--------------|----------------|-----------------|
| a_i | $2\sqrt{6}/3$ | $\sqrt{2}$ | $2\sqrt{10}/5$ | $2\sqrt{3}/3$ | 0 | $2\sqrt{3}/3$ | $\sqrt{6}/3$ | $\sqrt{10}/5$ | $2\sqrt{15}/15$ |
| c_i | $2\sqrt{6}$ | $5\sqrt{2}$ | $11\sqrt{10}/5$ | $5\sqrt{3}$ | 3 | $\sqrt{3}$ | $-\sqrt{6}$ | $3\sqrt{10}/5$ | $-3\sqrt{15}/5$ |
| d_i | $2\sqrt{6}$ | $5\sqrt{2}$ | $11\sqrt{10}/5$ | $5\sqrt{3}$ | -3 | $\sqrt{3}$ | $-\sqrt{6}$ | $3\sqrt{10}/5$ | $-3\sqrt{15}/5$ |
| e_i | $2\sqrt{6}/3$ | $\sqrt{2}$ | $2\sqrt{10}/5$ | $2\sqrt{3}/3$ | 1 | $-\sqrt{3}/3$ | $\sqrt{6}/3$ | $\sqrt{10}/5$ | $2\sqrt{15}/15$ |
| f_i | $2\sqrt{6}/3$ | $\sqrt{2}$ | $2\sqrt{10}/5$ | $2\sqrt{3}/3$ | -1 | $-\sqrt{3}/3$ | $\sqrt{6}/3$ | $\sqrt{10}/5$ | $2\sqrt{15}/15$ |

The hadronic currents in the standard model in the limit to take the weak and the electromagnetic coupling zero with the quark mass parameters zero is known to have a $U(N) \times U(N)$ symmetry where N is the number of the flavor [13]. If we switch on the quark mass parameters, this symmetry is badly broken; however, we find that there still exist the conserved quantum numbers such as charge, baryon number, strangeness, charm, bottom, top corresponding to the invariance under the global phase transformation. This means that the flavor groups such as $SU(4)$, $SU(5)$, and $SU(6)$ are useful for a classification of the hadrons as a natural extension of $SU(3)$. On the other hand, the current algebra for good-good components on the null plane makes the algebra of $U(N) \times U(N)$ symmetry even when the mass parameters are switched on. This is because the current algebra for good-good component based on the canonical quantization on the null plane needs no equation of motion. It is derived only by the good component of the quark field where the canonical anticommutation relation is assumed. These are the reasons why we can extend the previous analysis in $SU(3)$ to the higher symmetry in spite of the large symmetry breaking by the heavy quark masses.

Now all the sum rules (2)–(7) diverge if $\alpha_P(0) \geq 1$. Since meaningful results can be obtained only when we start from the finite sum rules, the sum rules (2)–(7) were generalized to the nonforward matrix elements and continued analytically to the forward matrix elements [8]. The point of this discussion lies in the assumption that the rightmost singularity in the complex n plane or J plane was given by the moving Pomeron such that

at some small t the trajectory satisfies $\alpha_P(t) < 1$. A simple moving pole given by Donnachie and Landshoff [6] satisfies this criterion and gives a phenomenologically good description of the high-energy hadron-hadron scattering; hence, we give the results in this case in the following. Since the kinematics of the nonforward matrix element is cumbersome, here we use the effective method to take $\alpha_P(0) = 1 + b - \epsilon$ with $b = 0.0808$ [9]. We first let ϵ approach b from above, and then after taking out the simple poles from the sum rule we take it to be zero. By this method we do not lose any generality, and always obtain the same results as in the non-forward case. Thus we take the leading high-energy behavior of $\{\sigma^{\pi^+P}(\nu) + \sigma^{\pi^-P}(\nu)\}$ as $\beta_{\pi N} s^{\alpha_P(0)-1} \beta_{\pi N}$ with $s = m_N^2 + m_\pi^2 + 2\nu$ and $\beta_{\pi N} = 70.0(1/\text{GeV})^2$, and similarly for the kaon with $\beta_{KN} = 60.7(1/\text{GeV})^2$. For the structure function we take

$$\{F_2^{\nu P}(x, Q^2) + F_2^{\nu P}(x, Q^2)\} \\ \sim (Q_0^2/Q^2)^{\alpha_P(0)-1} \beta_{\nu N}(Q^2, 1 - \alpha_P(0)) (2\nu)^{\alpha_P(0)-1} \\ \text{with } Q_0^2 = 1 \text{ GeV}^2, \text{ and } F_2^{eN}(x, Q^2) \text{ as}$$

$$(Q_0^2/Q^2)^{\alpha_P(0)-1} \beta_{eN}(Q^2, 1 - \alpha_P(0)) (2\nu)^{\alpha_P(0)-1}.$$

We expand β_{lN} with $l = \nu$ or e as

$$\beta_{lN}^0(Q^2) + (\epsilon - b)\beta_{lN}^1(Q^2) + O((\epsilon - b)^2).$$

Then we define

$$I_\pi = g_A^2(0) + \frac{2f_\pi^2}{\pi} \int_{\nu_0^\pi}^\infty \frac{d\nu}{\nu^2} \left\{ \sqrt{\nu^2 - m_N^2 m_\pi^2} [\sigma^{\pi^+P}(\nu) + \sigma^{\pi^-P}(\nu)] - \nu s^b \beta_{\pi N} \right\} + \frac{2f_\pi^2 \beta_{\pi N}}{\pi} \ln \left(\frac{1}{2\nu_0^\pi} \right), \quad (8)$$

$$I_K^p = [g_A^{p\Sigma^0}(0)]^2 + [g_A^{p\Lambda}(0)]^2 + \frac{2f_K^2}{\pi} \int_{\nu_0^K}^\infty \frac{d\nu}{\nu^2} \left\{ \sqrt{\nu^2 - m_K^2 m_N^2} [\sigma^{K^+P}(\nu) + \sigma^{K^-P}(\nu)] - \nu s^b \beta_{KN} \right\} \\ + \frac{2f_K^2 \beta_{KN}}{\pi} \ln \left(\frac{1}{2\nu_0^K} \right) + U_p, \quad (9)$$

$$I_K^n = [g_A^{n\Sigma^-}(0)]^2 + \frac{2f_K^2}{\pi} \int_{\nu_0^K}^\infty \frac{d\nu}{\nu^2} \left\{ \sqrt{\nu^2 - m_K^2 m_N^2} [\sigma^{K^+n}(\nu) + \sigma^{K^-n}(\nu)] - \nu s^b \beta_{KN} \right\} + \frac{2f_K^2 \beta_{KN}}{\pi} \ln \left(\frac{1}{2\nu_0^K} \right) + U_n, \quad (10)$$

$$C_p = \int_0^1 \frac{dx}{x} \{F_2^{ep}(x, Q^2) - x^{-b} \beta_{ep}^0(Q^2)\} - \beta_{ep}^1(Q^2), \quad (11)$$

$$C_n = \int_0^1 \frac{dx}{x} \{F_2^{en}(x, Q^2) - x^{-b} \beta_{en}^0(Q^2)\} - \beta_{en}^1(Q^2). \quad (12)$$

From the experimental data I_π , I_K^p , I_K^n are determined as $I_\pi \sim 5.17$, $I_K^p \sim 2.39$, $I_K^n \sim 1.61$ [14]. The regularization of the sum rules can be understood very simply in $SU(3)$. In this case we notice that the sum rules (2) and (3) are related directly. Then, by the above parametrization, from the coefficient of the simple pole we obtain

$\pi \beta_{\nu N}^0 = 4f_\pi^2 \beta_{\pi N}$, and after taking out these simple poles from the sum rule, we find that the finite part of it depends on $\beta_{\nu N}^1(Q^2)$. To remove this $\beta_{\nu N}^1(Q^2)$, we assume that the Pomeron term corresponds to the $A_0(\alpha, 0)$ term in the sum rule. By this assumption we obtain the relation $\beta_{\nu N}^0 = 6\beta_{ep}^0$, $\beta_{ep}^0 = \beta_{en}^0$, $\beta_{\nu N}^1 = 6\beta_{ep}^1$, $\beta_{ep}^1 = \beta_{en}^1$.

Now, once we recognize that the divergence of the sum rules comes from the $A_0(\alpha, 0)$ term, we can see that $C_p(C_n)$ in $SU(N)$ is different from the one in $SU(N+1)$. This is because the coefficient of $A_0(\alpha, 0)$ in $SU(N)$ is different from the one in $SU(N+1)$. Thus we add the suffix as $C_p^N(C_n^N)$ to express that it is the value in $SU(N)$. Thus we obtain

$$I_\pi - 3C_p^3 = \frac{1}{2}\{\tilde{F}_2^{\nu p} + \tilde{F}_2^{\nu p}\} - 6\tilde{F}_2^{ep}, \quad (13)$$

$$C_p^3 - C_n^3 = \tilde{F}_2^{ep} - \tilde{F}_2^{en}, \quad (14)$$

where \tilde{F}_2 is defined as

$$\tilde{F}_2 = \int_0^1 \frac{dx}{x} F_2(x, Q^2). \quad (15)$$

Similarly from the sum rule in the KN reactions, we obtain

$$\begin{aligned} I_K^p - 3C_p^3 &= I_K^n - 3C_n^3 \\ &= 3\{\tilde{F}_2^{ep} + \tilde{F}_2^{en}\} - \{\tilde{F}_2^{\nu p} + \tilde{F}_2^{\nu p}\}, \end{aligned} \quad (16)$$

together with the relation $f_\pi^2 \beta_{\pi N} = f_K^2 \beta_{KN}$. Note that \tilde{F}_2^{lN} always appear in the combination where the leading singularities which make each integral diverge cancel out. Thus on the right-hand side of the sum rules (13), (14), (16), every integral should be understood to be taken after this cancellation. Then these sum rules give us the relation

$$C_p^3 = \frac{1}{9}(2I_K^p - I_K^n + 2I_\pi), \quad (17)$$

$$C_p^3 - C_n^3 = \frac{1}{3}(I_K^p - I_K^n). \quad (18)$$

The sum rules (14) and (18) give us the modified Gottfried sum rule. Using the Adler-Weisberger sum rule for the kaon, we can express this as

$$\int_0^1 \frac{dx}{x} \{F_2^{ep}(x, Q^2) - F_2^{en}(x, Q^2)\} = \frac{1}{3} \left(1 - \frac{4f_K^2}{\pi} \int_{m_K m_N}^\infty \frac{d\nu}{\nu^2} \sqrt{\nu^2 - (m_K m_N)^2} \{ \sigma^{K^+n}(\nu) - \sigma^{K^+p}(\nu) \} \right). \quad (19)$$

In the parton language the sum rule (19) can be transformed as

$$\int_0^1 dx \{ \lambda_d(x, Q^2) - \lambda_u(x, Q^2) \} = 0.11, \quad (20)$$

and the sum rules (13) and (16) as

$$\int_0^1 dx \{ \lambda_d(x, Q^2) - \lambda_s(x, Q^2) \} = 0.89, \quad (21)$$

where $\lambda_i(x, Q^2)$ specifies the sea quark of the i quark. The constraints from the coefficients of the simple poles can be transformed as

$$\begin{aligned} \lim_{x \rightarrow 0} x^{\alpha P(0)} \lambda_u(x, Q^2) &= \lim_{x \rightarrow 0} x^{\alpha P(0)} \lambda_d(x, Q^2) \\ &= \lim_{x \rightarrow 0} x^{\alpha P(0)} \lambda_s(x, Q^2) = a \end{aligned} \quad (22)$$

with $a \sim 0.1$. For $SU(N)$ above $N = 4$, we use the fact that $[A_c(p \cdot x, x^2 = 0)]_{\alpha\beta}$ can be decomposed as $i f_{\alpha c \beta} F(p \cdot x, 0) + d_{\alpha c \beta} D(p \cdot x, 0)$ for $c \neq 0$, where α, β are the symmetry index specifying the octet hadronic state. In $SU(4)$ we obtain [15]

$$I_\pi - \frac{9}{5}C_p^4 = \frac{6}{5}\tilde{F}_2^{ep} - \frac{1}{8}(\tilde{F}_2^{\nu p} + \tilde{F}_2^{\nu p}), \quad (23)$$

$$I_K^p - \frac{9}{5}C_p^4 = \frac{2}{3}(\tilde{F}_2^{\nu p} + \tilde{F}_2^{\nu p}) - \frac{9}{5}\tilde{F}_2^{ep} - 3\tilde{F}_2^{en}, \quad (24)$$

$$C_p^4 = \frac{1}{9}(I_K^n + 4I_\pi), \quad (25)$$

$$\tilde{F}_2^{ep} - \tilde{F}_2^{en} = C_p^4 - C_n^4 = \frac{1}{3}(I_K^p - I_K^n), \quad (26)$$

and the symmetry relations $\pi \beta_{\nu N}^0 = 8 f_\pi^2 \beta_{\pi N}$ with $\beta_{\nu N}^0 = \frac{36}{5} \beta_{ep}^0$. Compared with $SU(3)$, $\beta_{\nu N}^0$ increases by $4 f_\pi^2 \beta_{\pi N}$.

We can understand this increase in the parton model easily. It simply means that

$$\lim_{x \rightarrow 0} x^{\alpha P(0)} \lambda_c(x, Q^2) = a. \quad (27)$$

Further we notice that there is a correspondence between the integral of the sea quark distribution and a certain combination of $\int_{-\infty}^\infty (d\alpha/\alpha) A_i(\alpha, 0)$. For example, for the strange sea quark in $SU(3)$, we have a correspondence [16]

$$\int_0^1 dx \lambda_s(x, Q^2) \iff \int_{-\infty}^\infty \frac{d\alpha}{\alpha} \left(\frac{\sqrt{6}}{6} A_0(\alpha, 0) - \frac{\sqrt{3}}{3} A_8(\alpha, 0) \right), \quad (28)$$

and, in $SU(4)$,

$$\int_0^1 dx \lambda_s(x, Q^2) \iff \int_{-\infty}^\infty \frac{d\alpha}{\alpha} \left(\frac{\sqrt{2}}{4} A_0(\alpha, 0) - \frac{\sqrt{3}}{3} A_8(\alpha, 0) + \frac{\sqrt{6}}{12} A_{15}(\alpha, 0) \right). \quad (29)$$

The structure of the matrix on the right-hand side of (28) is $\text{diag}(0, 0, 1)$, and that of (29) is $\text{diag}(0, 0, 1, 0)$ where $\text{diag}(\dots)$ means the diagonal matrix element. Since we take the matrix element of the nucleon, we find that the integral of the strange quark distribution in $SU(3)$ is the same as in $SU(4)$. Thus, by the extension of the flavor group from $SU(3)$ to $SU(4)$ we see that the $SU(3)$ part in $SU(4)$ is unchanged. This fact is more directly expressed in the sum rule (26). Here we see that the modified Gottfried sum rule takes the same form whether we consider it in $SU(3)$ or in $SU(4)$. Under this recognition we find that the sum rules (23) and (24) can be understood simply by the addition of the charm sea quark which has

a correspondence

$$\int_0^1 dx \lambda_c(x, Q^2) \iff \int_{-\infty}^{\infty} \frac{d\alpha}{\alpha} \left(\frac{\sqrt{2}}{4} A_0(\alpha, 0) - \frac{\sqrt{6}}{4} A_{15}(\alpha, 0) \right). \quad (30)$$

and that they are transformed to relations (20) and

$$\int_0^1 \{ \lambda_c(x, Q^2) - \lambda_s(x, Q^2) \} = 1.39. \quad (31)$$

Since $\lambda_u, \lambda_d, \lambda_s$ are the same as those in SU(3), we see that $(C_p^4 - C_p^3)$ gives us information on the charm sea quark where we have $C_p^3 = 1.50$ and $C_p^4 = 2.48$ from (17) and (25). Thus if we define

$$D = \int_0^1 dx \{ \lambda_d(x, Q^2) - ax^{-\alpha_P(0)} \}, \quad (32)$$

$$U = \int_0^1 dx \{ \lambda_u(x, Q^2) - ax^{-\alpha_P(0)} \}, \quad (33)$$

$$S = \int_0^1 dx \{ \lambda_s(x, Q^2) - ax^{-\alpha_P(0)} \}, \quad (34)$$

$$C = \int_0^1 dx \{ \lambda_c(x, Q^2) - ax^{-\alpha_P(0)} \}, \quad (35)$$

we obtain the constraint on C from $(C_p^4 - C_p^3)$, and from (20), (21), (31) on D, U, S as

$$\begin{aligned} D &= \frac{9}{20}\beta + 0.60, & U &= \frac{9}{20}\beta + 0.49, \\ S &= \frac{9}{20}\beta - 0.29, & C &= \frac{9}{20}\beta + 1.10, \end{aligned} \quad (36)$$

where β is β_{ep}^1 in SU(4). The same logic can be repeated by the extension from SU(4) to SU(5) and SU(5) to SU(6), and we find

$$B = \int_0^1 dx \{ \lambda_b(x, Q^2) - ax^{-\alpha_P(0)} \} = \frac{9}{20}\beta + 1.10, \quad (37)$$

$$T = \int_0^1 dx \{ \lambda_t(x, Q^2) - ax^{-\alpha_P(0)} \} = \frac{9}{20}\beta + 1.10, \quad (38)$$

where

$$\lim_{x \rightarrow 0} x^{\alpha_P(0)} \lambda_b(x, Q^2) = \lim_{x \rightarrow 0} x^{\alpha_P(0)} \lambda_t(x, Q^2) = a. \quad (39)$$

Detailed formula are given in Appendix B.

Now β enters all the sea quarks uniformly. Hence the following parton model sum rule for the isoscalar nucleon target can be obtained as

$$\begin{aligned} \int_0^1 dx F_3^{\nu N}(x, Q^2) &= \frac{1}{2} \int_0^1 dx \{ F_3^{\nu N}(x, Q^2) \\ &\quad + F_3^{\bar{\nu} N}(x, Q^2) \} - 2.78. \end{aligned} \quad (40)$$

The first term on the right-hand side of the sum rule (40) is roughly 3; hence, we will find that the left-hand side of it becomes roughly zero. This sum rule is β independent but needs experimental information in the very small x

region. Though the β dependence remains, the inequality $S < U < D < C \sim B \sim T$ holds. Hence we see that the heavy sea quarks exist abundantly. Since they are suppressed in the medium or the large x region, they should be confined in the small x region. Now, even at $Q^2 = 5 \text{ GeV}^2$, the threshold ν for the charm sea quark is $2\nu_{\text{th}} \sim 20 \text{ GeV}^2$.

Then the threshold x becomes $x_{\text{th}} \sim Q^2/2\nu_{\text{th}} \sim Q^2 \times 0.05 = 0.25$. Hence in the kinematical region below $x \sim 0.01$, it can be excited easily if it exists intrinsically in the proton. The same kind of fact holds true in the bottom sea quark case. On the other hand, a preliminary study based on the phenomenologically successful parameters in hadron physics together with the nonperturbative constraints explained here suggests that the charm and the bottom sea quarks become abundant below $x \sim 0.01$ even if they are suppressed greatly above $x \sim 0.1$ at low Q^2 . To show these facts in a concrete example we construct a toy model of the structure function F_2^{ep} in the next section. This model satisfies the various constraints obtained in this section which are based on the phenomenologically successful parameters in the hadron physics [6] and also takes into account the perturbative Q^2 dependence. This shows that abundant intrinsic heavy sea quarks may explain the steep rise of the structure function F_2^{ep} with decreasing x observed at HERA.

III. MATCHING THE PERTURBATIVE Q^2 DEPENDENCE TO THE NONPERTURBATIVE CONSTRAINTS

The structure function F_2 at low x is controlled by its moments at small n . Various constraints discussed in the previous section correspond to the ones at $n = 1$. As n becomes large, the moments will be dominated by the contribution given by the perturbative QCD [17]. Here we assume that the values of the moments above $n = 2$ can be given by this contribution. Let us explain this more. The integral of the parton distribution function introduced in the previous section is nothing but the decomposition of the moment of the structure function F_2 at $n = 1$ into the quantity which has a correct quantum number of each sea quark. Thus these are the physical quantity and are not necessarily the ones in the perturbative QCD. The difference lies in the nonperturbative dynamics. What we assume here is that the asymptotic behavior of these distributions is controlled by the soft Pomeron and not by the hard Pomeron. Even if the gluon in the perturbative sense gives the behavior of the hard Pomeron, we think that it should be screened by the nonperturbative dynamics in the hadron level. On the other hand, we assume that the moments of these distributions above $n = 2$ should coincide with the ones in the perturbative QCD. Thus we can expect that the gluon in the very small x region is completely different from the perturbative one, but as we go to the large x region it becomes similar to the perturbative ones. The latter should be observed as a rise of the F_2 as we go to the large Q^2 region. In our approach, the rapid rise in

the small x region should be explained not by the perturbative evolution but by the intrinsic heavy sea quarks. It goes without saying that the gluon is relevant to these sea quarks, but it is in the nonperturbative sense. Now among the moments of each sea quark given by the perturbative QCD, only the one at $n = 2$ is increasing with increasing Q^2 . In other words, a rise of the F_2 with increasing Q^2 at low x is controlled mainly by the moment at $n = 2$. Since such a rise is observed roughly below $x \sim 0.1$, we try to take into account a typical perturbative behavior below $x \sim 0.1$ by considering only the moment at $n = 2$. Thus our inputs are the following: The constraint in the $x \rightarrow 0$ limit given by (22), (27), and (39) with $a \sim 0.1$, where a is determined by the $\beta_{\pi N}$ in [6] through the sum rule. The nonperturbative constraint for each sea quark at $n = 1$ given by (36)–(38). The moment at $n = 2$ is given by the perturbative QCD. Then we parametrize each sea quark as

$$\lambda_i(x, Q^2) = (a + h_i x^\delta)(1-x)^{n_i}/x^{1+b}, \quad (41)$$

where $a = 0.1$, $b = 0.0808$, and $\delta = 0.5333$, and determine h_i and n_i to satisfy the above-mentioned constraints. Here we fix δ to agree with the next-to-leading order term in [6]. This is due to the fact that the complex n plane singularity at $n = \alpha$ corresponds to the J plane singularities at $J = \alpha, \alpha - 2, \dots$ [18]. As is clear, the distribution obtained in such a way can never be extrapolated above $x \sim 0.1$.

Now from (41), we obtain

$$\begin{aligned} \langle \tilde{\lambda}_i \rangle_1 &= \int_0^1 dx \left(\lambda_i(x, Q^2) - \frac{a}{x^{1+b}} \right) \\ &= \int_0^1 dx \frac{a\{(1-x)^{n_i} - 1\}}{x^{1+b}} + h_i B(1-k, n_i + 1), \end{aligned} \quad (42)$$

where $k = 1 + b - \delta$, and $B(a, b)$ is the β function. For the integer n_i we obtain

$$\begin{aligned} \Sigma(n_i) &= \int_0^1 dx \frac{a\{(1-x)^{n_i} - 1\}}{x^{1+b}} \\ &= -a \sum_{r=1}^{n_i} (r-1)! \frac{\Gamma(1-b)}{\Gamma(r+1-b)}. \end{aligned} \quad (43)$$

Since the right-hand side of (43) is a monotonically de-

creasing function with respect to n_i , for the noninteger n_i , we use the value determined by

$$\Sigma(n_i) = \Sigma([n_i]) + (n_i - [n_i])\{\Sigma([n_i] + 1) - \Sigma([n_i])\}, \quad (44)$$

where $[n_i]$ is the largest integer satisfying $[n_i] \leq n_i$. In terms of $\langle \tilde{\lambda}_i \rangle_1$, U , D , S , C , B , and T are expressed as $\langle \tilde{\lambda}_u \rangle_1$, $\langle \tilde{\lambda}_d \rangle_1$, $\langle \tilde{\lambda}_s \rangle_1$, $\langle \tilde{\lambda}_c \rangle_1$, $\langle \tilde{\lambda}_b \rangle_1$, and $\langle \tilde{\lambda}_t \rangle_1$, respectively. The moment at $n = 2$ is given by

$$\begin{aligned} \langle \lambda_i \rangle_2 &= \int_0^1 dx x \lambda_i(x, Q^2) \\ &= aB(1-b, n_i + 1) + h_i B(2-k, n_i + 1). \end{aligned} \quad (45)$$

Then from (42) and (45), we obtain

$$n_i = (1-k) \left(\frac{\{\langle \tilde{\lambda}_i \rangle_1 - \Sigma(n_i)\}}{\{\langle \lambda_i \rangle_2 - aB(1-b, n_i + 1)\}} - 1 \right) - 1, \quad (46)$$

$$\begin{aligned} h_i &= \frac{\{\langle \tilde{\lambda}_i \rangle_1 - \Sigma(n_i)\}}{B(1-k, n_i + 1)} \\ &= \frac{\{\langle \lambda_i \rangle_2 - aB(1-b, n_i + 1)\}}{B(2-k, n_i + 1)}. \end{aligned} \quad (47)$$

Thus, by giving the value $\langle \lambda_i \rangle_2$ we can numerically search the value n_i which satisfies (46), and once we find this, we can determine h_i by (47).

Let us discuss how we determine $\langle \lambda_i \rangle_2$. As already explained we use here the moment determined by the evolution equation in perturbative QCD. Since the purpose of this paper is not in the quantitative prediction but in the qualitative study to see how the nonperturbative constraints match the perturbative behavior, we use here the evolution at the one-loop order. However since the mass effect of the heavy quarks can be expected to be very large we take their effects approximately by using the momentum scheme procedure to set $M = Q$ in the Georgi-Politzer formula [19] where M is the scale parameter. Because the anomalous dimension γ_{tg} is proportional to Q^2/m_t^2 for $m_t \gg Q$, the evolution of the top quark can be neglected below $Q^2 \sim 1000 \text{ GeV}^2$ for the top quark mass parameter $m_t > 100 \text{ GeV}$. Hence we take the effective flavor number as 5. In this case, the massless evolution equation is

$$\langle \lambda_i(Q^2) \rangle_2 = \frac{1}{10} \langle q^s(Q^2) \rangle_2 + \frac{1}{10} \langle 10\lambda_i(Q_0^2) - q^s(Q_0^2) \rangle \exp(-d_2 s), \quad (48)$$

$$\langle q^s(Q^2) \rangle_2 = \{(1 - \alpha_2) \langle q^s(Q_0^2) \rangle_2 - \beta_2 \langle g(Q_0^2) \rangle_2\} \exp(-d_2^+ s) + \{\alpha_2 \langle q^s(Q_0^2) \rangle_2 + \beta_2 \langle g(Q_0^2) \rangle_2\} \exp(-d_2^- s), \quad (49)$$

where

$$\langle q^s \rangle_2 = \left\langle u_v + d_v + 2 \sum_{i=u,d,s,c,b} \lambda_i \right\rangle_2, \quad (50)$$

and $\langle g(Q^2) \rangle_n$ is the n th moment of the gluon distribution function at Q^2 , and $\alpha_2 = \beta_2 = 0.4839$, $d_2^+ = 0.8986$, $d_2^- = 0$, $d_2 = 0.4638$. Here the antiquark distribution is included by assuming $\lambda_i = \lambda_{\bar{i}}$. To take the mass effect of the charm and the bottom, we calculate the second moment of them by the equations

$$\langle \lambda_c(Q^2) \rangle_2 = \langle \lambda_c(Q_0^2) \rangle_2 - \frac{1}{10} \langle g(Q_0^2) \rangle_2 \int_{Q_0}^Q \frac{dM}{M} \gamma_{cg}^2, \quad (51)$$

$$\langle \lambda_b(Q^2) \rangle_2 = \langle \lambda_b(Q_0^2) \rangle_2 - \frac{1}{10} \langle g(Q_0^2) \rangle_2 \int_{Q_0}^Q \frac{dM}{M} \gamma_{bg}^2, \quad (52)$$

where we consider the evolution only through the gluon and keep the term only up to order g^2 . The anomalous dimension of γ_{ig}^2 and the effective coupling g^2 are given in [19] as

$$\begin{aligned} \gamma_{ig}^2 = & \frac{-5g^2}{4\pi^2} \left[\frac{1}{3} + \frac{m^4}{M^4} \frac{4}{\sqrt{1+4m_i^2/M^2}} \ln \left(\frac{\sqrt{1+4m_i^2/M^2}-1}{\sqrt{1+4m_i^2/M^2}+1} \right) + \frac{4m_i^4}{M^4} \frac{1}{1+4m_i^2/M^2} \right. \\ & \left. - \frac{4m_i^6}{M^6} \frac{2}{(1+4m_i^2/M^2)^{3/2}} \ln \left(\frac{\sqrt{1+4m_i^2/M^2}-1}{\sqrt{1+4m_i^2/M^2}+1} \right) \right] \end{aligned} \quad (53)$$

and

$$\begin{aligned} \frac{1}{g^2(M^2)} = & \frac{1}{g^2(Q_0^2)} + \frac{1}{8\pi^2} \left\{ \left(11 - \frac{2}{3}f \right) \ln \left(\frac{M}{Q_0} \right) + \frac{2}{3} \sum_j \left[\ln \left(\frac{M}{Q_0} \right) - \frac{2m_j^2}{M^2} + \frac{2m_j^2}{Q_0^2} \right. \right. \\ & \left. \left. + \frac{1}{2} \left(\frac{2m_j^2}{M^2} - 1 \right) \sqrt{1 + \frac{4m_j^2}{M^2}} \ln \left(\frac{\sqrt{1+4m_j^2/M^2}+1}{\sqrt{1+4m_j^2/M^2}-1} \right) \right. \right. \\ & \left. \left. - \frac{1}{2} \left(\frac{2m_j^2}{Q_0^2} - 1 \right) \sqrt{1 + \frac{4m_j^2}{Q_0^2}} \ln \left(\frac{\sqrt{1+4m_j^2/Q_0^2}+1}{\sqrt{1+4m_j^2/Q_0^2}-1} \right) \right] \right\}, \end{aligned} \quad (54)$$

where the explicit integrations are done. Here we take $m_c = 1.5$ GeV and $m_b = 4.5$ GeV, and $g^2(Q_0^2) \sim 4.266$ by setting $\Lambda = 0.2$ GeV and $Q_0^2 = 5$ GeV². The moments $\langle \lambda_c(Q^2) \rangle_2$ and $\langle \lambda_b(Q^2) \rangle_2$ calculated by (51) and (52) are, in general, overestimated; however, compared with those calculated by the massless evolution, they are suppressed enough up to some Q^2 . Hence, as a measure of the mass effect, we use $\langle \lambda_c(Q^2) \rangle_2$ and $\langle \lambda_b(Q^2) \rangle_2$ determined by (51) and (52) until they become larger than those determined by (48).

Initial values of the valence quarks are $\langle u_v(Q_0^2) \rangle_2 = 0.2706$, $\langle u_v(Q_0^2) \rangle_3 = 0.08558$, $\langle d_v(Q_0^2) \rangle_2 = 0.1074$, and $\langle d_v(Q_0^2) \rangle_3 = 0.02668$. Initial values of the sea quarks are constrained by $\langle \tilde{\lambda}_i \rangle_1$. These $\langle \tilde{\lambda}_i \rangle_1$ depend on β , and this β in general depends on Q^2 . The important fact is that this β enters uniformly all the sea quarks. Thus experimental information of the up and the down sea quarks can in general restrict the allowed value of β . For example, an extremely large $|\beta|$ can be excluded. However we do not have enough experimental information yet to investigate such a restriction. We just know through the experimental value of the Gottfried sum rule that they are asymmetric. Further we do not have theoretical information yet of this β . Thus we studied the distribution $\tilde{\beta} = \frac{9}{20}\beta = 0, 0.2, 0.4, \text{ and } 0.6$ by fixing the perturbative evolution. The set of parameters $\{n_i, h_i\}$ at $Q_0^2 = 5$ GeV² for $\tilde{\beta} = 0$ are given in Table II. We also give these parameters for other values of $\tilde{\beta}$. In these cases the scale Q^2 is not clear as explained above.

Here we first set the value n_i , and then determine h_i by

$\langle \tilde{\lambda}_i \rangle_1$. The second moments $\langle \lambda_i \rangle_2$ and $\langle g \rangle_2$ under these initial values are also given. As is clear from the table, n_d, n_u, n_s for the different values of $\tilde{\beta}$ are chosen to keep the second moments at roughly a constant value. It goes without saying that such a restriction can be relaxed and that here we have a large freedom to choose parameters. Initial values of n_c and n_b are taken large to express the threshold effect due to their masses effectively.

TABLE II. Parameters n_i, h_i for the input sea quark distributions.

| $\tilde{\beta}$ | 0 | 0.2 | 0.4 | 0.6 |
|-------------------------------|-----------------------|-----------------------|-----------------------|-----------------------|
| n_d | 15.0 | 18.0 | 21.0 | 24.0 |
| h_d | 1.75 | 2.33 | 2.94 | 3.60 |
| $\langle \lambda_d \rangle_2$ | 3.54×10^{-2} | 3.52×10^{-2} | 3.50×10^{-2} | 3.48×10^{-2} |
| n_u | 18.0 | 22.0 | 26.0 | 29.0 |
| h_u | 1.73 | 2.36 | 3.05 | 3.71 |
| $\langle \lambda_u \rangle_2$ | 2.80×10^{-2} | 2.76×10^{-2} | 2.73×10^{-2} | 2.79×10^{-2} |
| n_s | 40.0 | 60.0 | 80.0 | 100 |
| h_s | 0.623 | 1.59 | 2.71 | 3.94 |
| $\langle \lambda_s \rangle_2$ | 5.96×10^{-3} | 5.98×10^{-3} | 5.90×10^{-3} | 5.86×10^{-3} |
| n_c | 300 | 300 | 300 | 300 |
| h_c | 13.0 | 14.4 | 15.7 | 17.1 |
| $\langle \lambda_c \rangle_2$ | 3.46×10^{-3} | 3.77×10^{-3} | 4.06×10^{-3} | 4.37×10^{-3} |
| n_b | 500 | 500 | 500 | 500 |
| h_b | 17.2 | 18.9 | 20.6 | 22.3 |
| $\langle \lambda_b \rangle_2$ | 2.17×10^{-3} | 2.35×10^{-3} | 2.53×10^{-3} | 2.71×10^{-3} |
| $\langle g^2 \rangle_2$ | 0.528 | 0.528 | 0.528 | 0.529 |
| $\langle g \rangle_2$ | 0.472 | 0.472 | 0.472 | 0.471 |

TABLE III. Parameters n_t, h_t for the input top quark distributions.

| n_t | 10000 | 3000 | 5000 | 10 000 |
|-------------------------------|-----------------------|-----------------------|-----------------------|-----------------------|
| h_t | 24.9 | 45.0 | 59.2 | 86.0 |
| $\langle \lambda_t \rangle_2$ | 1.16×10^{-3} | 4.27×10^{-4} | 2.79×10^{-4} | 1.08×10^{-4} |

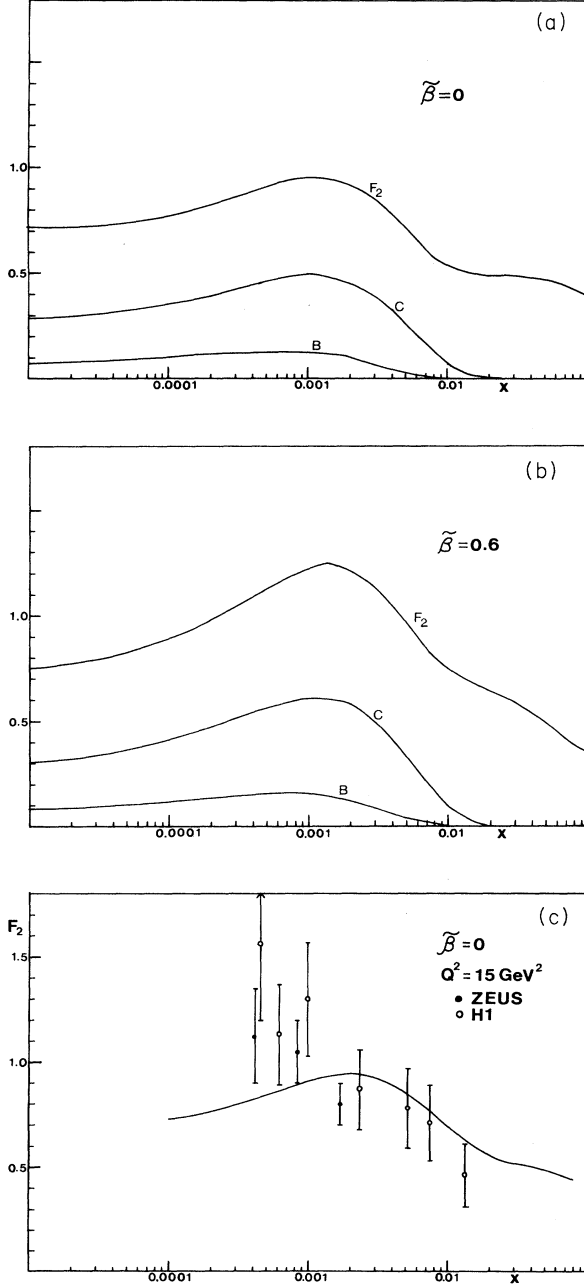


FIG. 1. The structure function F_2 as a function of x for $\tilde{\beta} = 0$ at $Q^2 = 5 \text{ GeV}^2$. A charm sea quark component (C) and a bottom sea quark one (B) in F_2 are also given where the antiquark contribution is included by assuming $\lambda_i = \lambda_{\bar{i}}$. (b) The same as (a) for $\tilde{\beta} = 0.6$. (c) The structure function F_2 without the top quark for $\tilde{\beta} = 0$ at $Q^2 = 15 \text{ GeV}^2$, where HERA's data are plotted for the comparison.

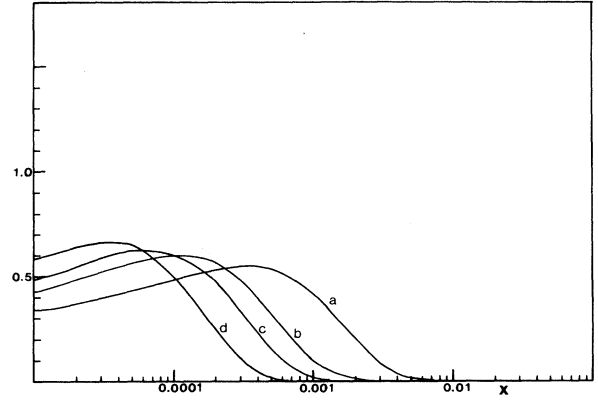


FIG. 2. A top sea quark component in F_2 for $\tilde{\beta} = 0$ in the cases $n_t = 1000$ (a), 3000 (b), 5000 (c), 10 000 (d), where the top-antiquark contribution is included by assuming $\lambda_t = \lambda_{\bar{t}}$.

Further n_c and n_b are fixed for the different value of $\tilde{\beta}$ since the variation of the second moments together with their magnitude are small by this fixing. Now the mass of the top quark is very large. If $m_t = 150 \text{ GeV}$, the threshold ν is $2\nu_{\text{th}} \sim (300)^2 \text{ GeV}^2$. Then the threshold x is $x \sim Q^2/(300)^2 \sim Q^2 \times 10^{-5}$, and we obtain $x_{\text{th}} \sim 5 \times 10^{-5}$ for $Q^2 = 5 \text{ GeV}^2$ and $x_{\text{th}} \sim 0.01$ for $Q^2 = 1000 \text{ GeV}^2$. Thus x_{th} lies in the kinematical region of HERA where we are most interested. Since the top quark is abundant as shown in Sec. II, once x becomes smaller than x_{th} , we can expect that its contribution rapidly becomes large. As an example of this fact, we give the top quark distributions for various values of n_t . Table III summarizes the parameters n_t and h_t for $\tilde{\beta} = 0$.

The structure function F_2 for $\tilde{\beta} = 0$ and $\tilde{\beta} = 0.6$ without the top quark contribution is given in Figs. 1(a) and 1(b), respectively. Here we also give the charm and the bottom contributions. Figure 1(c) is given for comparison with HERA's data as a typical example. The top quark contribution to F_2 is given in Fig. 2. A typical Q^2 dependence of F_2 due to the perturbative QCD for $\tilde{\beta} = 0$ is given in Fig. 3 at the various values of x , where the

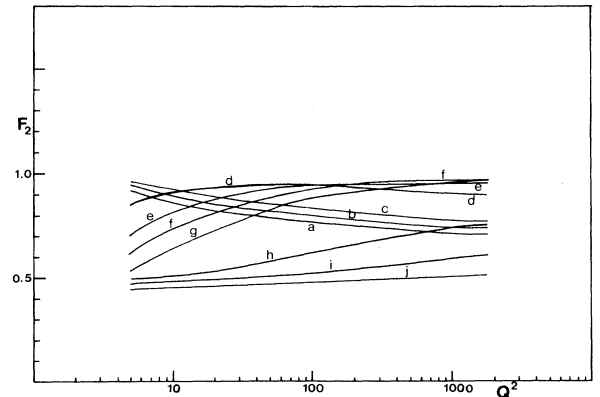


FIG. 3. Q^2 dependence of F_2 for $\tilde{\beta} = 0$ in the cases $x = 0.0005$ (a), 0.0007 (b), 0.001 (c), 0.003 (d), 0.005 (e), 0.007 (f), 0.01 (g), 0.03 (h), 0.05 (i), 0.07 (j).

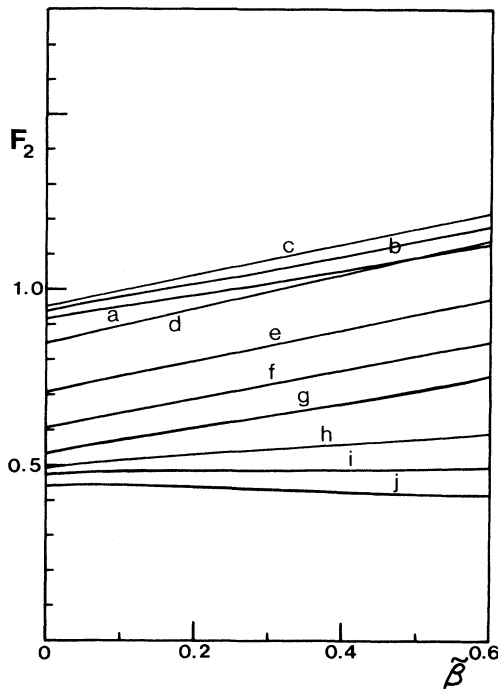


FIG. 4. $\tilde{\beta}$ dependence of F_2 at the same values as those in Fig. 3.

top quark contribution is not included. Figure 4 gives the $\tilde{\beta}$ dependence of F_2 without the top quark also at the various values of x .

From Figs. 1-4 we see the following.

(1) Below $x = 1 \times 10^{-3}$ for the fixed $\tilde{\beta}$ without the top quark, F_2 is decreasing with increasing Q^2 .

(2) Above $x = 1 \times 10^{-3}$ for fixed $\tilde{\beta}$ without the top quark, F_2 first increases with increasing Q^2 , but at a certain Q^2 it turns to decrease. This turning point increases with increasing x . Further, the slope of the increase becomes slow as we go to the large x value near $x \sim 0.1$.

(3) Below $x \sim 0.01$, F_2 increases with increasing $\tilde{\beta}$. The slope first increases with decreasing x , but below $x \sim 0.001$ it gradually becomes slow.

(4) The top quark contribution may become very large in the region $1 \times 10^{-4} \leq x \leq 1 \times 10^{-3}$. The effect of this will be seen as a steep rise of F_2 with a strong Q^2 dependence.

We can understand these properties as follows. At small Q^2 , the heavy sea quarks are confined in the small x region. Hence they appear as a steep rise of F_2 below $x \sim 0.01$. As Q^2 increases, the perturbatively produced (extrinsic) sea quarks spread over the larger x region. Because $\langle \tilde{\lambda}_i \rangle_1$ is kept constant for a fixed $\tilde{\beta}$, the bump of the sea quark distribution becomes broad with its peak flattened. Further, to keep the value $\tilde{\beta}$ at a constant value, the extrinsic sea quark cannot increase unboundedly. This is why we encounter the turning point with increasing Q^2 . Since the perturbative effect becomes dominant as we go to the larger x region, this turning point increases with increasing x . If we change $\tilde{\beta}$, we see that F_2 increases with increasing $\tilde{\beta}$ because the magnitude of

the bump is controlled by this value. Now to construct a realistic distribution, the extrinsic Q^2 dependence should be superimposed on the nonperturbative Q^2 dependence of $\tilde{\beta}$. Further we should add the top quark contribution which may produce a strong Q^2 dependence. We have not yet performed such an analysis since we do not know how $\tilde{\beta}$ depends on Q^2 . However we can see the qualitative behavior by comparing Figs. 1-4. For example, if F_2 increases with increasing Q^2 in the region $5 \times 10^{-4} \leq x \leq 1 \times 10^{-3}$ for $Q^2 \leq 50 \text{ GeV}^2$, it means that the increase of F_2 from the Q^2 dependence of $\tilde{\beta}$ overwhelms the decrease of it from the extrinsic Q^2 dependence for the fixed $\tilde{\beta}$ since the top quark is probably below its threshold. Finally we should comment on the stop of the rapid rise below $x \sim 0.001$ in Figs. 1(a)-1(c). As is stated frequently, in these figures, the contribution from the top quark is not included. Thus there should be a rise below $x < 0.001$ in our approach as stated in (4). It is not yet clear from what value of x such a rise begins. Model distributions for various parameters in Fig. 2 will give us some hint. We see that this rise will add up to about 0.5-0.6 to F_2 in Figs. 1(a)-1(c). As already discussed, the threshold x for the top quark excitation can be given roughly by $x_{\text{th}} \sim Q^2 \times 10^{-5}$ for $m_t = 150 \text{ GeV}$. Hence for high Q^2 above 100 GeV^2 , we will see a continuous rise of F_2 below $x < 0.001$. However, for low Q^2 we may encounter a dip-bump structure here. Whether or not such a structure exists depends crucially on the parameter δ which controls the value x of the position of the peak in Figs. 1(a)-1(c) and 2. In this paper we do not try to change this parameter. Rather we follow the one in [6] based on the discussion in a complex n plane. Further the change of $\tilde{\beta}$ can cause the scale up of F_2 . These facts together with the large experimental errors below $x \sim 0.001$ make the situation ambiguous. Thus the best we can say is that the intrinsic charm and the bottom quarks can explain the rapid rise in the region $0.001 < x < 0.01$ and that below $x < 0.001$ though we still can observe a rise due to the top quark, its magnitude and the structure of F_2 in this region are ambiguous.

IV. DISCUSSIONS

The Q^2 dependence of the structure function F_2 at low x is complex because both the perturbative and the nonperturbative Q^2 dependences exist. The nonperturbative Q^2 dependence originates from the structure of the Pomeron. The perturbative one is severely restricted by the nonperturbative constraints, and we will have a turning point such that for a fixed x above $x = 0.001$ the rise of F_2 with increasing Q^2 changes to decrease. The value of Q^2 of this turning point is decreasing with decreasing x , though the effect may be obscured by the nonperturbative Q^2 dependence. The phenomenon is similar to the shadowing [20] but its dynamical origin is heavily related to abundance of intrinsic heavy sea quarks, which in turn is related to the spontaneous chiral symmetry breaking of the vacuum. The important difference from the shadowing in [20] is that in our case the saturation limit as

$x \rightarrow 0$ is Q^2 independent.

Our analysis in this paper is based on the standard model with the three generations, hence if the particles other than the ones in the standard model exist below or near the top quark mass, our result will change. Within the standard model, to get the quantitative prediction we have many things to do. First of all, we need the theory to determine the explicit Q^2 dependence of β . This will be equivalent to know the Pomeron in QCD. Next we should reduce the free parameters concerned with the sea quarks. The sum rule for $F_3^{\nu N}$ for the isoscalar nucleon target will be helpful in this respect. For example, the sum rule (40) suggests that we investigate the quantity

$$\begin{aligned} I(x_0) &= \int_{x_0}^1 dx F_3^{\nu N} - \frac{1}{2} \int_{x_0}^1 dx \{F_3^{\nu N} + F_3^{\bar{\nu} N}\} \\ &= 2 \int_{x_0}^1 dx \{\lambda_s(x, Q^2) - \lambda_c(x, Q^2)\} \\ &\quad + 2 \int_{x_0}^1 dx \{\lambda_b(x, Q^2) - \lambda_t(x, Q^2)\}. \end{aligned} \quad (55)$$

A typical behavior of $I(x_0)$ in our toy model at $Q^2 = 5, 15, 54 \text{ GeV}^2$ for $\tilde{\beta} = 0$ is given in Fig. 5. Here we neglect the contribution to $I(x_0)$ from the region above $x = 0.1$ and use the top quark distribution of $n_t = 10000$. We will first see a small rise in the region $0.01 \leq x \leq 0.1$ due to the strange quark. Then the flattening or decrease by the charm quark follows. Once the bottom quark begins to contribute, $I(x_0)$ increases rapidly and finally it turns to decrease by the top quark and converges to the asymptotic value -2.78 . Such a large dip-bump structure with a large negative asymptotic value is typical of our model. In the case of perturbative QCD without intrinsic heavy sea quarks, at low Q^2 such as 5 GeV^2 we will encounter the monotonic increasing behavior as we go to the small x since only the strange sea quark contributes to the right-hand side of (55). Even if we take into account the charm sea quark, since it will be produced only through the gluon, its magnitude will be very small in such a low Q^2 region. Hence we will again see the monotonic increasing behavior. If Q^2 becomes large, extrinsic heavy sea quarks are produced rapidly. In such a case we will see a dip-bump

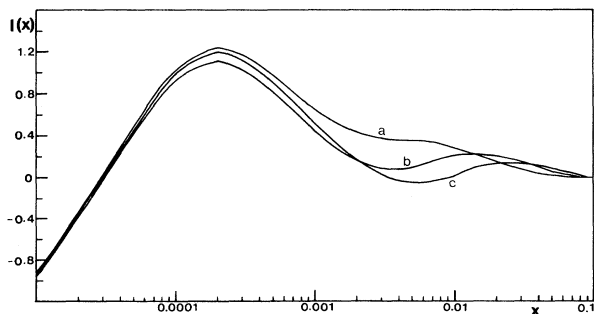


FIG. 5. $I(x_0)$ as a function of x_0 for $Q^2 = 5$ (a), 15 (b), 54 (c) GeV^2 where the contribution above $x = 0.1$ is neglected.

structure, but such a behavior is pushed to the smaller x region compared with our case because of the mass suppression effect in the anomalous dimensions. Further the asymptotic value will not take a large asymmetric value since the gluon is flavor singlet. The fact that in our case the asymptotic value is negative comes from the fact $T \sim B \sim C \gg S$. The origin of this large asymmetry lies in the spontaneous chiral symmetry breaking of the vacuum.

From phenomenology, there is an indication to suggest existence of the intrinsic heavy sea quark. Many years ago, the existence of the hard intrinsic charm quark was suggested [21], and from then this model has been considered one of the most hopeful candidates to account for the charm production data at low p_\perp in the large x_f region [22]. A recent experiment by E769 strongly supports this picture [23]. Though the intrinsic component suggested in this model will have little effect on $C = \langle \tilde{\lambda}_c \rangle_1$ since this value is dominated by the contribution from the small x region, it surely gives us the idea that the intrinsic heavy sea quark is not a strange thing. Moreover the hard intrinsic component [21] may be dynamically related to our abundant intrinsic component at low x by some mechanism. The existence of such a mechanism which relates the low-energy region to the high-energy one is one of the most important physical messages from the modified Gottfried sum rule [8,9,24]. This is the physics suggested by Weinberg many years ago [25]. In Appendix C we give another discussion which suggests the existence of such a mechanism.

APPENDIX A

The derivation of relation (1) breaks up into two parts. The first part is the derivation of the Deser-Gilbert-Sudarshan (DGS) representation of the current anticommutator. The second part is the study of the condition to restrict it to the null plane. We explain these parts step by step in the following. The DGS representation itself is not popular these days, however, we first give a brief review of its derivation focusing on the spectral condition which plays an important role in these discussions.

Step (0): A review of the DGS representation [11]. Let us take a scalar current $J_a(x)$, and consider the integral representation of the matrix element of the current commutator between the stable one-particle state defined as

$$\begin{aligned} \tilde{C}_{ab}(x^2, p \cdot x) &= \langle p | [J_a(x), J_b(0)] | p \rangle_c \\ &= \int d\alpha d\beta \exp[i(\alpha x^2 + \beta p \cdot x)] G_{ab}(\alpha, \beta). \end{aligned} \quad (A1)$$

Since the current commutator is zero for the spacelike separation, G_{ab} is analytic in the lower half-plane in a complex α plane. Expressing this analyticity as

$$G_{ab}(\alpha, \beta) = \int_0^\infty d\lambda^2 \exp(i\lambda^2/4\alpha) \tilde{H}_{ab}(\lambda^2, \beta), \quad (\text{A2})$$

and introducing the Hilbert transform of \tilde{H}_{ab} as

$$\tilde{H}_{ab}(\lambda^2, \tilde{\beta}) = P \int d\beta \frac{1}{\tilde{\beta} - \beta} h_{ab}(\lambda^2, \beta), \quad (\text{A3})$$

it is straightforward to show

$$\begin{aligned} C_{ab}(p \cdot q, q^2) &= \int d^4x \exp(iq \cdot x) \tilde{C}_{ab}(x^2, p \cdot x) \\ &= 2\pi \int_0^\infty d\lambda^2 \int d\beta \delta((q + \beta p)^2 - \lambda^2) \epsilon(q^0 + \beta p^0) h_{ab}(\lambda^2, \beta). \end{aligned} \quad (\text{A5})$$

Let us now consider the support property of the weight function h_{ab} . Any physical vector satisfies $(p \cdot q)^2 \geq m^2 q^2$, where $p^2 = m^2$. We take the set of points satisfying this condition as the universal set Ω . The s -channel physical region is $s = (p + q)^2 \geq M_s^2$ and the u channel is $u = (p - q)^2 \geq M_u^2$. We call the union of the s -channel and the u -channel physical regions as \bar{R} , and its complement with respect to Ω as R . For any point in R , if the integration path in the (β, λ^2) plane determined by the δ function in (A5) exists, h_{ab} must be zero there. Thus, by taking a union of the lines for all points in R , we can see in what region of β the weight function should be zero. For this purpose we first define σ as $\sigma = \lambda^2 - \beta^2 m^2$, and consider a set of paths generated by $\sigma = 2\beta(p \cdot q) + q^2$ and $(p \cdot q)^2 = m^2 q^2$. The condition for these two curves in the $(p \cdot q, q^2)$ plane being tangent to each other is $\sigma = -\beta^2 m^2$. This parabola plays a very important role. The integration path for any point in the set Ω intersects or is tangent to the parabola. The condition $\lambda^2 \geq 0$ required by causality corresponds to $\sigma \geq -\beta^2 m^2$. The point determined by

$$\begin{aligned} \tilde{C}_{ab}(x^2, p \cdot x) &= \int_0^\infty d\lambda^2 \int d\beta \exp(i\beta p \cdot x) h_{ab}(\lambda^2, \beta) i\Delta(x, \lambda^2), \end{aligned} \quad (\text{A4})$$

where numerical factors are absorbed in h_{ab} . The momentum space representation of \tilde{C}_{ab} becomes

the sign function where it changes its sign always lies in the causality forbidden region $\sigma < -\beta^2 m^2$. The next step is to search the region where the integration path exists for the points in R . We first note that the path always passes the point $\beta_0 = -q^2/(2p \cdot q)$ for $p \cdot q \neq 0$. Let us take the s -channel boundary. At this point $\beta_0 = 1 - (M_s^2 - m^2)/(-q^2 + M_s^2 - m^2)$. Since $M_s > m$, $0 \leq \beta_0 \leq 1$ for $q^2 \leq 0$. On the one hand, $\sigma = M_s^2 - m^2$ at $\beta = 1$. Thus we see that the paths for $p \cdot q > 0, q^2 < 0$ in R sweeps the region $\beta > 1$. For $q^2 > 0$, since $(p \cdot q)^2 \geq m^2 q^2$, q^2 is bounded as $q^2 \leq (M_s - m)^2$ at the s -channel boundary. Thus by using the fact that the path always intersects or is tangent to the parabola $\sigma = -\beta^2 m^2$, the region $\sigma \leq 2m(m - M_s)\beta + (m - M_s)^2$ is swept by the point in R . Applying the same kind of discussion to the u -channel boundary, we finally find that the support of the weight function lies at least in the regions $-1 \leq \beta \leq 1$ and $\sigma \geq \min[(M_s - m)^2, (M_u - m)^2] > 0$.

Step (1): Derivation of the DGS representation of the current anticommutator. Let us decompose the C_{ab} as

$$C_{ab}(p \cdot q, q^2) = \sum_n (2\pi)^4 \delta^4(p + q - n) \langle p | J_a(0) | n \rangle \langle n | J_b(0) | p \rangle - \sum_n (2\pi)^4 \delta^4(p - q - n) \langle p | J_b(0) | n \rangle \langle n | J_a(0) | p \rangle. \quad (\text{A6})$$

By taking a frame at rest, $p = (m, 0)$, we see that the first and the second terms are disconnected under the assumption $m < (M_s + M_u)/2$. On the other hand, in the s channel where $p \cdot q > 0$, the path $\sigma = 2\beta(p \cdot q) + q^2$ intersects the support of the weight function only in the region where $\epsilon(q^0 + \beta p^0) = 1$. This is because the sign change occurs only in the region $\sigma < -\beta^2 m^2 < 0$. Hence we obtain [11,26]

$$2\pi \int_0^\infty d\lambda^2 \int_{-1}^1 d\beta \delta((q + \beta p)^2 - \lambda^2) h_{ab}(\lambda^2, \beta) \theta(q^0 + \beta p^0) = \sum_n (2\pi)^4 \delta^4(p + q - n) \langle p | J_a(0) | n \rangle \langle n | J_a(0) | p \rangle. \quad (\text{A7})$$

By the same kind of discussion in the u channel we obtain

$$2\pi \int_0^\infty d\lambda^2 \int_{-1}^1 d\beta \delta((q + \beta p)^2 - \lambda^2) h_{ab}(\lambda^2, \beta) \theta(-(q^0 + \beta p^0)) = \sum_n (2\pi)^4 \delta^4(p - q - n) \langle p | J_b(0) | n \rangle \langle n | J_a(0) | p \rangle. \quad (\text{A8})$$

Equations (62) and (63) give us the DGS representation of the current anticommutator as

$$\begin{aligned} W_{ab}(p \cdot q, q^2) &= \int d^4x \exp(iq \cdot x) \langle p | \{J_a(x), J_b(0)\} | p \rangle_c \\ &= 2\pi \int_0^\infty d\lambda^2 \int_{-1}^1 d\beta \delta((q + \beta p)^2 - \lambda^2) h_{ab}(\lambda^2, \beta). \end{aligned} \quad (\text{A9})$$

Step (2): Restriction of the current anticommutator to the null plane. Restriction to the null plane can be done by the integration over q^- with some assumption for the weight function. To investigate this assumption we consider

$$I_{ab} = \lim_{\Lambda \rightarrow \infty} \int_{-\infty}^{\infty} dq^- \exp(-(q^-)^2/\Lambda^2) H_{ab}(p \cdot q, q^2), \quad (\text{A10})$$

where H_{ab} denotes C_{ab} or W_{ab} . Here we replace the sign function $\varepsilon(q^0 + \beta p^0)$ in C_{ab} by $\varepsilon(q^+ + \beta p^+)$ appropriate to the null-plane formalism. Since the constraint $(q + \beta p)^2 - \lambda^2 = 0$ is linear with respect to q^- , no constraint on β and λ^2 can be obtained by the integration over q^- . Then we consider under what condition on the weight function we can take the limit $\Lambda \rightarrow \infty$. Since $p^+ > 0$ and q^+ are arbitrary parameters, we take $q^+/p^+ > 1$. In this case the sign change occurs at $\beta < -1$. Since the point of this sign change always lies in the region $\sigma < -\beta^2 m^2$ and since the integration path $\sigma = 2\beta(p \cdot q) + q^2$ always intersects the parabola, it passes the support of the weight function only in the case $p \cdot q > 0$. Thus we can safely set $\varepsilon(q^+ + \beta p^+) = 1$. The same kind of thing holds for the case $q^+/p^+ < -1$, where in this case $p \cdot q < 0$. After all we find that the weight function should be $h_{ab}(\lambda^2, \beta) \sim \lambda^{-2-\varepsilon}$ as $\lambda \rightarrow \infty$, where ε is an arbitrary positive number. Since this constraint has no dependence on p and q , it must hold irrespective of the constraint $|q^+/p^+| > 1$. Then where is the difference between the current commutator and the anticommutator? We have investigated only the right-hand side of (A5) and (A9). In order to get the fixed-mass sum rule we introduce another assumption on the left-hand side of them. We integrate W_{ab} or C_{ab} over q^- and change the variable from q^- to $\nu = p \cdot q$. Then q^2 becomes

$$q^2 = 2 \left(\frac{q^+}{p^+} \right) (\nu - p^- q^+ + p^\perp \bar{q}^\perp) - (\bar{q}^\perp)^2. \quad (\text{A11})$$

Now the fixed-mass sum rule can be obtained by assuming that ν integration and setting $q^+ = 0$ can be interchanged. If this is allowed, q^2 becomes $-(\bar{q}^\perp)^2$. However, as is clear in (A11), q^2 can take positive values above some ν_0 for $q^+/p^+ > 0$. Hence, to allow for this interchange, we must assume that contributions from the positive q^2 regions are zero. Since $\nu_0 \rightarrow \infty$ as $q^+ \rightarrow 0$, this condition becomes the one as $\nu \rightarrow \infty$ and is called a superconvergence relation. It is at this point where the difference between the current commutator and the anticommutator appears.

Let us move to the vector current or the axial-vector current. In this case the DGS representation has many terms corresponding to different tensor structures. However, all the discussions in the scalar current case can be applied. A new feature appears when we are restricted to the null plane. Let us consider the good-good component which is equivalent to take the tensor $\mu\nu$ as $++$. On the null plane, the DGS representation of the current commutator has many terms which have no counterpart in the usual current algebra. Hence, by assuming this algebra

on the null plane, we get one equation which expresses the fact that these parts are zero. This equation contains the sign function $\varepsilon(q^+ + \beta p^+)$. However, as discussed when we derive the condition for the DGS representation to be restricted to the null plane, if we take $(q^+/p^+) > 1$ we can set $\varepsilon(q^+ + \beta p^+) = 1$. By repeating the same kind of reasoning there, we find that the equation where the sign function is replaced by 1 holds except at $q^+ = 0$. Then, since the limit $q^+ \rightarrow 0$ is the correct one to reach the fixed-mass sum rule, we can understand the value at $q^+ = 0$ by this limiting value. Thus we find that in the current anticommutator the terms corresponding to the ones which are zero in the current commutator are also zero. In this way we reach relation (1).

APPENDIX B

(B-1): The sum rule for SU(5). In this case a piece of the charged weak current corresponding to the third generation is absent and the Cabibbo-Kobayashi-Maskawa angles $|V_{ub}|$ and $|V_{cb}|$ are very small and can be set zero. In this approximation we obtain the symmetry relation $\pi\beta_{\nu N}^0 = 8f_\pi^2\beta_{\pi N} = \frac{72}{11}\beta_{ep}^0$ and the sum rules

$$I_\pi - \frac{18}{11}C_p^5 = \frac{15}{11}\tilde{F}_2^{ep} - \frac{3}{7}\tilde{F}_2^{en} - \frac{1}{7}(\tilde{F}_2^{\nu p} + \tilde{F}_2^{\nu p}), \quad (\text{B1})$$

$$I_K^p - \frac{18}{11}C_p^5 = \frac{9}{14}(\tilde{F}_2^{\nu p} + \tilde{F}_2^{\nu p}) - \frac{18}{11}\tilde{F}_2^{ep} - \frac{18}{7}\tilde{F}_2^{en}, \quad (\text{B2})$$

$$\tilde{F}_2^{ep} - \tilde{F}_2^{en} = C_p^5 - C_n^5 = \frac{1}{3}(I_K^p - I_K^n). \quad (\text{B3})$$

Thus, we find $C_p^5 = 2.72$ and $C_n^5 = 2.46$.

(B-2): The sum rule for SU(6). The symmetry relation is $\pi\beta_{\nu N}^0 = 12f_\pi^2\beta_{\pi N}$ with $\beta_{\nu N}^0 = \frac{36}{5}\beta_{ep}^0$. The sum rules are

$$I_\pi - \frac{6}{5}C_p^6 = \frac{9}{5}\tilde{F}_2^{ep} - \tilde{F}_2^{en} - \frac{1}{9}(\tilde{F}_2^{\nu p} + \tilde{F}_2^{\nu p}), \quad (\text{B4})$$

$$I_K^p - \frac{6}{5}C_p^6 = \frac{13}{18}(\tilde{F}_2^{\nu p} + \tilde{F}_2^{\nu p}) - \frac{6}{5}\tilde{F}_2^{ep} - 4\tilde{F}_2^{en}, \quad (\text{B5})$$

$$\tilde{F}_2^{ep} - \tilde{F}_2^{en} = C_p^6 - C_n^6 = \frac{1}{3}(I_K^p - I_K^n). \quad (\text{B6})$$

Thus, we find $C_p^6 = 3.70$ and $C_n^6 = 3.44$.

APPENDIX C

Here we consider the sum rules for SU(3) and consider the effect of the SU(3) symmetry breaking on the symmetry relations. Now if we look into the modified Gottfried sum rule (19), we notice that it depends only on the quantity $P \int_{-\infty}^{\infty} (d\alpha/\alpha) A_3(\alpha, 0)$. On the other hand, the relation $f_\pi^2\beta_{\pi N} = f_K^2\beta_{KN}$ obtained by the flavor singlet assumption seems to be violated at the 10–20% level. The deviation of the value of the Gottfried sum from a naively expected value $\frac{1}{3}$ is at the 20% level. Hence it is important to make clear how far we can relax this flavor singlet assumption.

Let us set

$$\widetilde{A}_0(\alpha, 0) = A_0(\alpha, 0) \cos \theta + A_8(\alpha, 0) \sin \theta ,$$

$$\pi\beta_{\nu N} = 4f_\pi^2\beta_{\pi N} , \quad (C2)$$

$$\widetilde{A}_8(\alpha, 0) = -A_0(\alpha, 0) \sin \theta + A_8(\alpha, 0) \cos \theta , \quad (C1)$$

$$\frac{f_\pi^2 \beta_{\pi N}}{f_K^2 \beta_{KN}} = \frac{2(\sqrt{2} \cos \theta + \sin \theta)}{2\sqrt{2} \cos \theta - \sin \theta} , \quad (C3)$$

and assume the contribution of the Pomeron is given by the term $\widetilde{A}_0(\alpha, 0)$. In other words, we consider that the residue of the Pomeron has an SU(3) symmetry-breaking piece. Then by comparing the coefficient of $P \int_{-\infty}^{\infty} (d\alpha/\alpha) \widetilde{A}_0(\alpha, 0)$ in each of the sum rules, we obtain the relations

$$\frac{3\beta_{ep}}{2\sqrt{2} \cos \theta + \sin \theta} = \frac{\beta_{\nu N}}{4(\sqrt{2} \cos \theta + \sin \theta)} . \quad (C4)$$

By using these relations, we obtain

$$I_\pi - \frac{6(\sqrt{2} \cos \theta + \sin \theta)}{2\sqrt{2} \cos \theta + \sin \theta} C_p^3 = \int_0^1 \frac{dx}{2x} \left[F_2^{\nu p} + F_2^{\nu p} - \frac{12(\sqrt{2} \cos \theta + \sin \theta)}{2\sqrt{2} \cos \theta + \sin \theta} F_2^{ep} \right] , \quad (C5)$$

$$I_K^p - \frac{3(2\sqrt{2} \cos \theta - \sin \theta)}{2\sqrt{2} \cos \theta + \sin \theta} C_p^3 = \int_0^1 \frac{dx}{x} \left[6F_2^{ep} + 3F_2^{en} - F_2^{\nu p} - F_2^{\nu p} - \frac{3(2\sqrt{2} \cos \theta - \sin \theta)}{2\sqrt{2} \cos \theta + \sin \theta} F_2^{ep} \right] , \quad (C6)$$

$$I_K^n - \frac{3(2\sqrt{2} \cos \theta - \sin \theta)}{2\sqrt{2} \cos \theta + \sin \theta} C_n^3 = \int_0^1 \frac{dx}{x} \left[6F_2^{en} + 3F_2^{ep} - F_2^{\nu p} - F_2^{\nu p} - \frac{3(2\sqrt{2} \cos \theta - \sin \theta)}{2\sqrt{2} \cos \theta + \sin \theta} F_2^{en} \right] , \quad (C7)$$

These sum rules give us the relations

$$C_p^3 = \frac{1}{9}(2I_\pi + 2I_K^p - I_K^n) , \quad C_n^3 = \frac{1}{9}(2I_\pi - I_K^p + 2I_K^n) . \quad (C8)$$

Thus we find that not only the modified Gottfried sum rule but also the values of C_p^3 and C_n^3 are the same as in the case $\theta = 0^\circ$. Further by using the experimental values, we obtain $\theta \sim -13^\circ$. In this case the sea quarks need some modifications. Though we define the mixing angle the same way as in the mixing angle of the singlet and octet pseudoscalar mesons, it is rather a surprise that it takes roughly the same value with the same sign as the canonical value of this mixing angle. In other words, the mixing angle in our case exactly re-

fects the Gell-Mann–Okubo mass relation. This is the reflection of the following facts. The lightlike axial charge does not commute with the generator P^- because of its nonconservation. Thus the mass operator P^2 does not commute with the lightlike axial charge, and the mass spectrum of the hadron in general contains a chiral non-singlet piece. This makes it possible to mix the singlet and the octet. On the other hand, the nonconservation of the lightlike charge is essential to the divergence of the sum rule which is related to the Pomeron. Concerned with this, Weinberg gave a very interesting discussion by using the pion-coupling matrix which is very similar to the lightlike axial charge [25]. In the SU(2) \times SU(2) model, he related the existence of the Pomeron to the fact that the hadron mass spectrum has a piece transforming like the fourth component of a chiral four-vector.

- [1] H1 Collaboration, I. Apt *et al.*, Nucl. Phys. **B407**, 515 (1993); H1 Collaboration, I. Apt *et al.*, Phys. Lett. B **321**, 161 (1994); ZEUS Collaboration, M. Derrick *et al.*, *ibid.* **316**, 412 (1993); ZEUS Collaboration, M. Derrick *et al.*, *ibid.* **332**, 228 (1994).
- [2] E. A. Kuraev, L. N. Lipatov, and V. S. Fadin, Sov. Phys. JETP **45**, 199 (1977); Ya. Ya. Balitsky and L. N. Lipatov, Sov. J. Nucl. Phys. **28**, 822 (1978).
- [3] A. J. Askew, J. Kwieciński, A. D. Martin, and P. J. Sutton, Phys. Rev. D **49**, 4402 (1994), and references cited therein.
- [4] A. D. Martin, W. J. Stirling, and R. G. Robert, Phys. Lett. B **306**, 135 (1993).
- [5] A. J. Askew, K. Golec-Biernat, J. Kwieciński, A. D. Mar-

- tin, and P. J. Sutton, Phys. Lett. B **325**, 212 (1994).
- [6] A. Donnachie and P. V. Landshoff, Phys. Lett. B **296**, 227 (1992).
- [7] S. Koretune, Phys. Lett. **83B**, 218 (1979); Phys. Rev. D **21**, 820 (1980); Phys. Lett. **113B**, 335 (1982).
- [8] S. Koretune, Prog. Theor. Phys. **72**, 821 (1984).
- [9] S. Koretune, Phys. Rev. D **47**, 2690 (1993). It should be noted that the modified Gottfried sum rule does not depend largely on the nuclear effects such as the shadowing and the meson exchange current. If the experimental value of the Gottfried sum changes by these effects, it simply means that we should properly take these effects into account when we extract the Kn total cross section data from the experiment. However since the energy re-

- gion which gives the main contribution to the integral of $(F_2^{ep} - F_2^{en})$ and the one of $(\sigma_{Kn} - \sigma_{Kp})$ is different, it may pose an interesting problem in nuclear effects.
- [10] E. Levin and C.-I. Tan, in *Proceedings of the XXII International Symposium on Multiparticle Dynamics*, Santiago de Compostela, Spain, 1992, edited by C. Pajares (World Scientific, Singapore, 1993), p. 568.
- [11] S. Deser, W. Gilbert, and E. C. G. Sudarshan, *Phys. Rev.* **115**, 731 (1959).
- [12] D. A. Dicus, R. Jackiw, and V. L. Teplitz, *Phys. Rev. D* **4**, 1733 (1971).
- [13] S. Weinberg, *Phys. Rev. D* **8**, 4482 (1973).
- [14] The values I_π, I_K^p, I_K^n are different from those given in [9]. This is because we used the recent high-energy data in their evaluation. However the value $(I_K^p - I_K^n)$ is unchanged since in its evaluation we had already used the recent high-energy data.
- [15] S. Koretune, *Prog. Theor. Phys.* **88**, 63 (1992).
- [16] This correspondence is not an exact one since the singlet component surely diverges and needs regularization as explained in the text. The integral of the parton distribution becomes Q^2 dependent due to this regularization. Then by adding the appropriate Q^2 -dependent piece to cancel the one from the integral, the correspondence here becomes exact. For example, see (11) and (12).
- [17] D. J. Gross and F. Wilczek, *Phys. Rev. D* **8**, 3633 (1973); **9**, 980 (1974); H. Georgi and H. D. Politzer, *ibid.* **9**, 416 (1974).
- [18] D. Z. Freedman and J. M. Wang, *Phys. Rev.* **160**, 1560 (1967); S. Koretune, *Prog. Theor. Phys.* **69**, 1746 (1983); **70**, 1170E (1983).
- [19] H. Georgi and H. D. Politzer, *Phys. Rev. D* **14**, 1829 (1976).
- [20] L. V. Gribov, E. M. Levin, and M. G. Ryskin, *Nucl. Phys.* **B188**, 555 (1983).
- [21] S. J. Brodsky, P. Hoyer, C. Peterson, and N. Sakai, *Phys. Lett.* **93B**, 451 (1980).
- [22] R. Vogt, S. J. Brodsky, and P. Hoyer, *Nucl. Phys.* **B383**, 643 (1992).
- [23] Fermilab E769 Collaboration, G. A. Alves *et al.*, *Phys. Rev. Lett.* **72**, 812 (1994).
- [24] S. Koretune, *Prog. Theor. Phys.* **89**, 1027 (1993); **90**, 1049 (1993).
- [25] S. Weinberg, in *Lectures on Elementary Particles and Quantum Field Theory*, edited by S. Deser, M. Grisaru, and H. Pendelton (MIT Press, Cambridge, MA, 1970), p. 283.
- [26] J. M. Cornwall, *Phys. Rev. D* **5**, 2868 (1972).